Surface Panel Method for Installed Multiple Rotor Flows

Walter O. Valarezo*
Douglas Aircraft Company, Long Beach, California 90846

A surface panel method capable of computing the flow on and about arbitrary multiple rotor propellers is presented. The complex rotor-to-rotor aerodynamic interaction is handled by computing time-averaged flows for each rotor and using a superposition technique to account for all rotor influences. The various features of the method are described, and computed results for multiple rotor configurations are presented for both isolated and installed cases. Comparisons to experimental data show good agreement and are presented wherever available. The multiple-rotor/airplane interference solutions presented are a first in the industry.

Nomenclature

A = total disk area
C_T, C_P = thrust and power coefficients, respectively
D = propeller diameter
J = advance ratio, U_∞/nD
n = revolutions per unit time
q_∞ = freestream dynamic pressure
T = net thrust

Introduction

EMPHASIS over the last decade on improving fuel efficiency for commercial transport aircraft has sparked renewed interest in the use of propellers as propulsive devices. Research and development efforts by propeller manufacturers have yielded significant advances in propeller technology, as evidenced by the propfan propeller concept. The propfan is a many-bladed, highly loaded propeller designed to operate efficiently in a high subsonic forward speed environment. Swirl energy recovery considerations have dictated that these new advanced propellers have counter-rotating tandem rotors. Efficient integration of this type of propulsive device with the remainder of the airframe has proven to be a formidable challenge to the aircraft aerodynamicist. Traditionally, it has generally been sufficient for aerodynamic integration purposes to treat a turbofan engine as a "black box" with specified inlet flow conditions. This approach is not sufficient for detailed design work for a propeller-powered airplane incorporating the new high-disk-loading propellers. Here, the propeller and aircraft flowfields are strongly coupled and neither can be treated as a black box. Because the propeller is unshrouded, the aerodynamicist requires predictive tools that can model the aircraft geometry and the propeller itself to produce optimized designs prior to wind-tunnel verification. From a computational point of view, proper modeling of these flows represents the most difficult challenge yet in the commercial transport business: highly complex geometries, relative motions, general unsteady effects, transonic flows, separated flows, and multienergy effects. Although it is clear that it would be highly desirable for the three-dimensional prediction methods to model all of these effects (full Navier-Stokes capability), a review of the literature indicates that this computational capability will not soon be available and may not even be in development. Meanwhile, both Boeing and McDonnell Douglas full-scale propfan demonstrator aircraft have already flown; the McDonnell Douglas aerodynamicists have relied considerably on the judicious use of timely developed panel method technology for the integration effort.

Various Euler solutions have been presented for single and counter-rotating propellers,[1-5] and recently a surface panel method for tandem rotors was presented.[6] All of these methods deal only with the isolated nacelle/propeller geometry. Although this capability should be of interest to the blade designer, it is not sufficient to address the propeller-airframe interference problem. The work presented in this paper is an extension of the propeller[7] and the time-averaging propeller/airframe[8] surface panel method capability developed at Douglas Aircraft over the last several years. The present method is currently inviscid; however, it could be linked to any suitable viscous capabilities through either a displaced surface or surface-blowing approach. The machinery for surface-blowing viscous corrections is already in the method. Coding the computational machinery for a displaced surface approach would be relatively trivial. The present method is also applicable to the installed tractor propeller problem and details of that development can be found in Ref. 9.

Multple-Rotor Procedure

A detailed description of the basic propeller panel method can be found in Ref. 7 and will not be repeated here. However, a brief description will be included for completeness. As in any panel method, the surface of the three-dimensional body to be analyzed is discretized into a large number of quadrilateral panels, as shown in Fig. 1 (only a fraction of the wake is displayed here for clarity). Source and dipole distributions are placed on the paneled surface and adjusted to satisfy the boundary conditions. The method uses a surface source technique where the source densities are adjusted to satisfy a zero normal velocity boundary condition on the exterior of the surface, and the dipole distribution is used to produce lift. Trailing vortex wakes issue from trailing edges of lifting sections of the body. An equal pressure Kutta condition is enforced at the trailing edges. In addition to the paneled "near" wakes, the method uses a surprisingly accurate far-wake approximation that significantly reduces computational effort.

The present method can handle any number of rotors by computing the flow on and due to each rotor sequentially and combining all rotor contributions at any point in the field. It is well known that the flow over a single rotor immersed in an axisymmetric onset can be considered steady in a blade-fixed coordinate system. However, for a counter-rotation configuration, the flow is unsteady in any reference frame at any condition. The present method does not attempt to solve this complex flow situation rigorously but rather decomposes the

Presented as Paper 89-2214 at the AIAA 27th Applied Aerodynamics Conference, Seattle, WA, July 31-Aug. 2, 1989; received Aug. 19, 1989; revision received June 16, 1990; accepted for publication June 20, 1990.

*Senior Engineer/Scientist, Aerodynamics Technology. Senior Member AIAA.

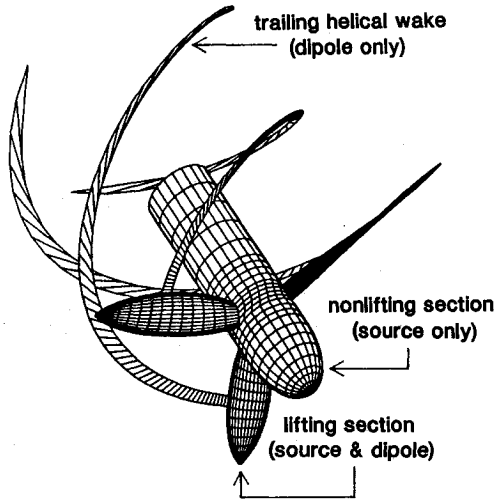

Fig. 1 Propeller panel method.

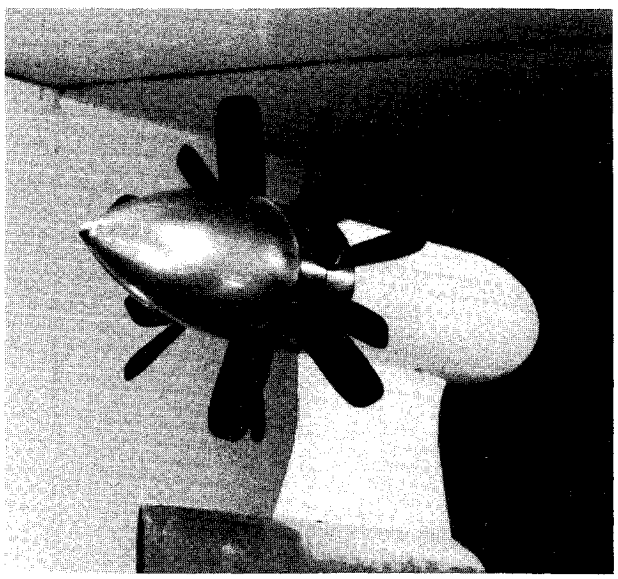

Fig. 2 Counter-rotating propeller.

unsteadiness introduced by the relative rotor motion into time-averaged influences due to each of the moving rotors. The computer flowfield at each rotor due to any other rotor is harmonically decomposed into its frequency content and the zeroth harmonic is utilized as the time-averaged onset to the propeller. The procedure is set up such that higher harmonics might be considered in fully unsteady analysis in the future. Contributions from any number of rotors at any other rotor are simply added as provided for by superposition. A specified number of rotor-to-rotor interaction iterations are performed.

Counter-Rotation Results

Calculations were conducted for the counter-rotating model shown in Fig. 2. The calculational procedure described in the previous section will now be illustrated step by step; it is noted here these steps are performed automatically by the code and are transparent to the user. First, onset velocities are provided as initial onset flows at rakes of field points corresponding to the two rotor disk locations, as shown in Fig. 3. These initial onset flows can be quite general and may include influences due to angle of attack, other aerodynamic surfaces, wing wakes, etc. This initial onset flow is decomposed harmonically and the zeroth harmonic is used in the present calculations; therefore, the flow can be nonuniform but it is rendered axisymmetric. The flow solution on the first rotor is then computed in the presence of this initial onset, and influences due

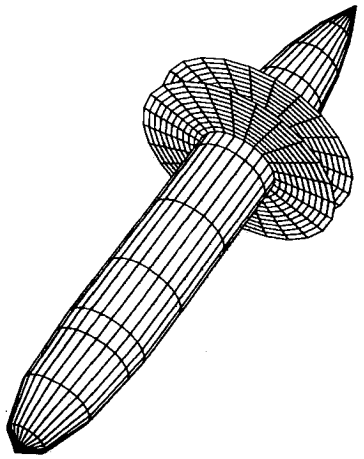

Fig. 3 Flowfield rakes.

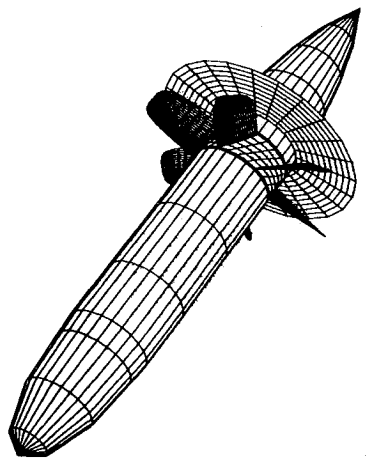

Fig. 4 Forward rotor and aft flowfield rake.

to the first rotor on the aft rotor are computed by interrogating the flow at the second rotor location, as shown in Fig. 4. This influence field is harmonically analyzed and the zeroth harmonic is added to the initial onset for the second rotor, and a flow solution for the aft rotor is then obtained. Again, the flow due to the aft rotor on the front rotor is sampled, as shown in Fig. 5, to update the onset flow to the front rotor. The steps just illustrated constitute one rotor-to-rotor interaction iteration, and good convergence has been obtained after four iterations. For the present calculations, the overall solution was judged to have converged when total thrust changed by 1% between iterations. The full counter-rotation geometry is shown in Fig. 6.

The problem of tracking wakes issuing from the front rotor that impinge on the aft rotor is avoided by simply terminating the "paneled" wakes a short distance after each of the rotors and using the analytical far-wake model described in Ref. 7. This far-wake model has been found to be accurate,[7] is computationally efficient, and allows for the termination of the physically paneled wakes early on so that they cannot collide with any downstream surfaces and, thus, introduce numerical and modeling problems. No assessment has been made to quantify the effects of time-dependent wake-blade interactions as the current procedure only addresses the zeroth-order harmonic (time-averaged) response.

Thrust loading and propeller efficiency curves are shown in Figs. 7 and 8, respectively. The computed results show good overall agreement with the experimental data. A converged solution for each advance ratio case requires approximately 15 CPU min on an IBM 3090 computer for the geometry of Fig. 6. This particular geometry has 5400 panels just on the surface of the blades. Figures 9 and 10 show how thrust and efficiency

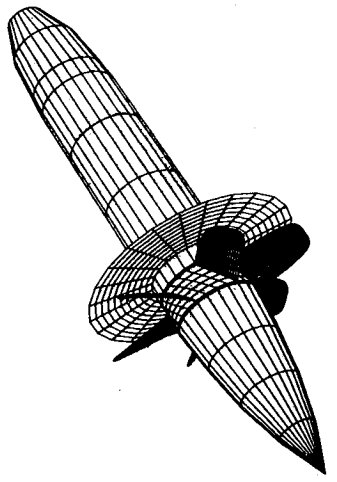

Fig. 5 Aft rotor and forward flowfield rake.

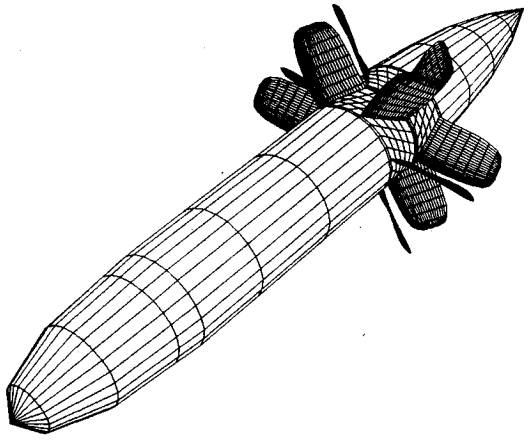

Fig. 6 Paneled counter-rotating propeller.

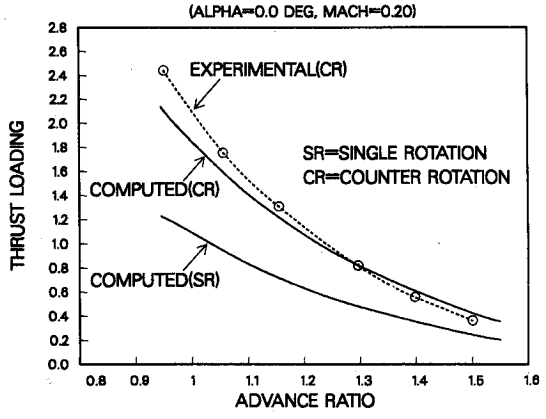

Fig. 7 Computed vs experimental thrust loading.

vary with advance ratio for each rotor, as computed by the method (no equivalent experimental data were available). It is interesting to note how the front rotor is generating significantly more thrust than the aft rotor over most of the advance ratio range and that its efficiency is adversely affected by the presence of the aft rotor as evidenced by the single-rotor results. This is explained by the fact that, for the counter-rotating propeller, each of the rotors is operating at a higher equivalent advance ratio than the single-rotor propeller due to the convective axial acceleration of the flow induced by either rotor. Since the blade pitch angles are all the same, the previously mentioned effect leads to reduced thrust levels for the individual rotors of the tandem configuration. Incidentally, the

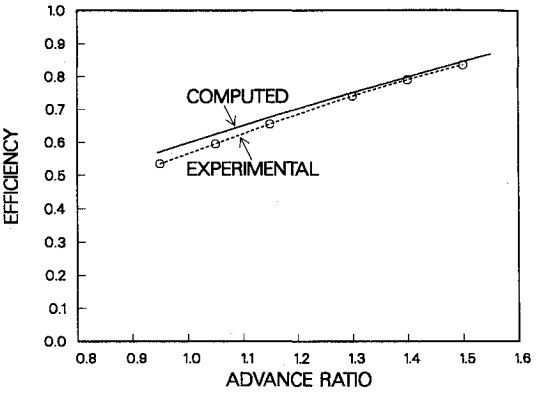

Fig. 8 Computed vs experimental efficiency.

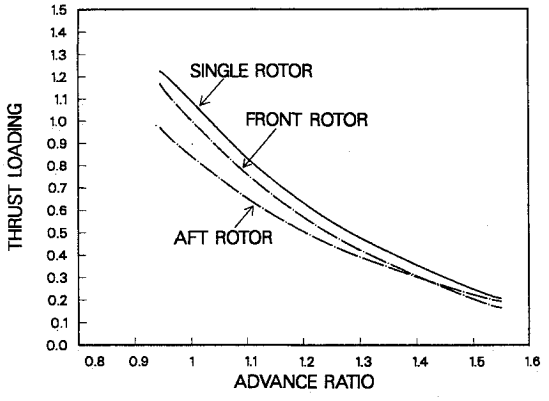

Fig. 9 Thrust loading split between rotors.

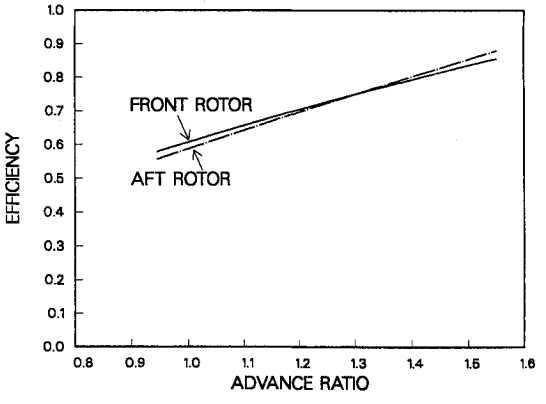

Fig. 10 Efficiency split between rotors.

comparisons of Figs. 7–10 were all performed at the same blade pitch angle (39 deg) for identical blade geometries.

Any Number of Rotors

The method was designed to be general enough so that any number of rotors could be analyzed. For example, Fig. 11 shows a four-rotor configuration derived from the counter-rotating propeller for the sake of convenience (same blade pitch and geometry). The method, however, can handle rotors that differ from one another in shape, panel number, blade number, rotation direction, and angular speed; in fact, it can easily handle rotor-stator combinations, if so desired. The four-rotor configuration also converged to a solution after four cycles. Figure 12 shows computed thrust loading and efficiency as a function of the number of rotors. All rotors are operating at a nominal advance ratio of 1.10. The computed solution indicated that the aft two rotors were, in fact, not generating very much thrust for this generic four-rotor geome-

try where all the rotors were set at the same blade pitch angle. This clearly would not be an optimum configuration.

Propeller/Airframe Interference

Propfan installation effects on full aircraft geometries have been successfully investigated computationally[10-12] using the method of Ref. 8. For these studies, the counter-rotating propulsor was simulated by running a single rotor geometrically situated midway between the front and aft rotor locations. A given total thrust (derived from wind-tunnel measurements) was then specified for the single rotor to match the total thrust for the tandem rotor arrangement. The code then iterated on rotor rpm until the desired thrust was attained. This technique of matching total propeller thrust has yielded remarkable agreement between computed and experimental propeller effects on candidate aircraft configurations (Fig. 13). This particular wind-tunnel configuration is shown without a tail, as is customary for tests not geared to obtain stability and control characteristics.

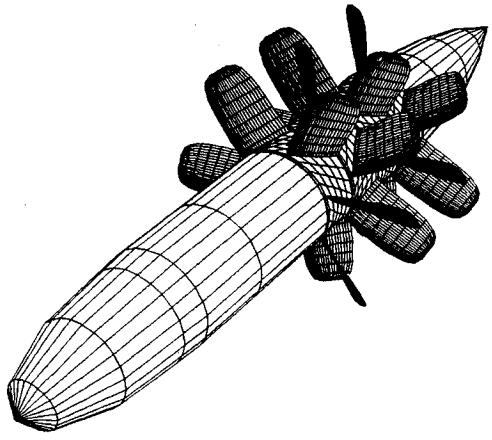

Fig. 11 Four-rotor geometry.

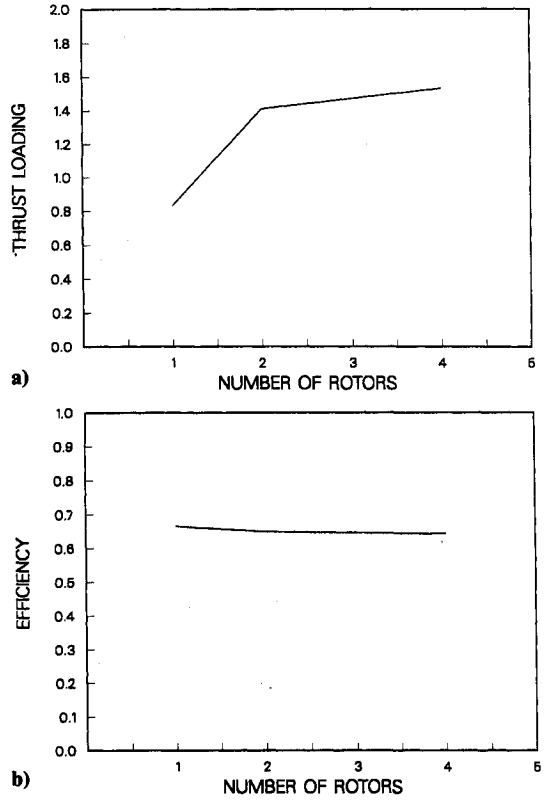

Fig. 12 Performance vs number of rotors: a) thrust loading; b) efficiency.

The time-averaging technique for off-body flowfields of Ref. 8 has been extended to take advantage of the new multiple-rotor capability. Thus, the real tandem propeller geometry and the complete aircraft geometry can be included in the analysis. Furthermore, any steady aerodynamic effects that might be a function of the spacing between rotors can now be studied numerically and accounted for in the propeller/airframe integration effort.

The wind-tunnel model corresponding to the geometry of Fig. 13 had counter-rotating propellers and can now be modeled, as shown in Fig. 14, with the present method. The wind-tunnel geometry was a 9% scale model of a proposed Douglas transport and was tested at atmospheric conditions. This geometry has close to 9000 panels on the half-body, and a complete solution was obtained in under 45 min of CPU time on an IBM 3090. Some of the detail of the paneling is revealed in Fig. 14b. The present method allows for the reduction of user input information to the bare essentials: paneled geometries, angle of attack, and advance ratios for each of the rotors. Thus, the user is not burdened with having to know what in reality is part of the answer, for example, thrust distributions across the propeller disk or any other resulting flow characteristic. Figure 15 shows the computed results for the full tandem rotor/aircraft geometry of Fig. 14 at the same nominal conditions as those of Fig. 13. The increments in fuselage surface

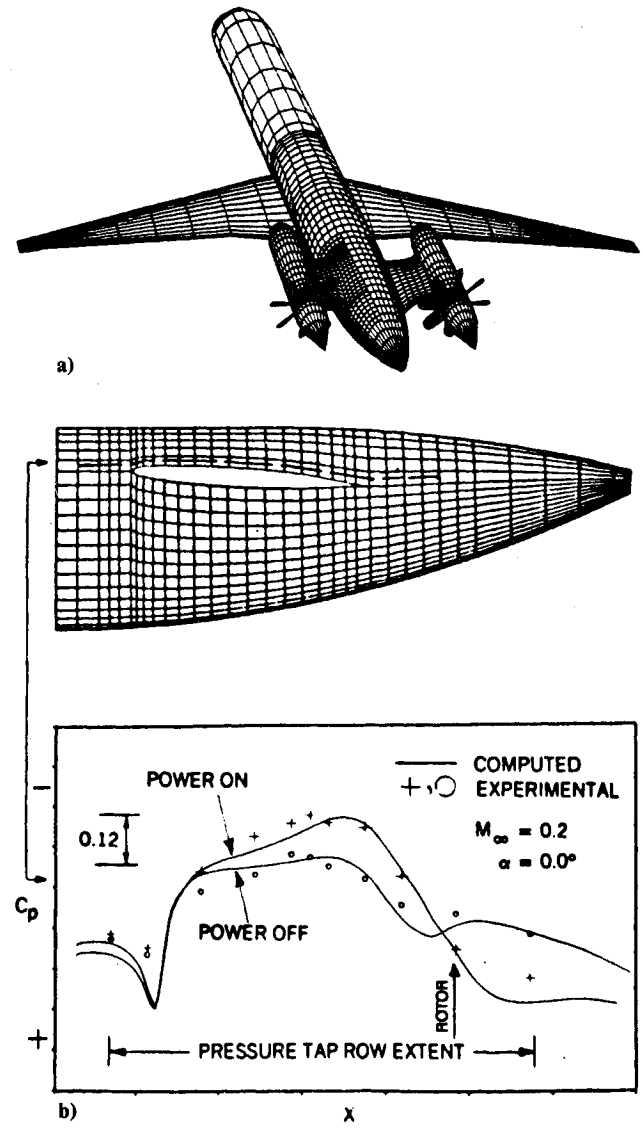

Fig. 13 Single-rotor simulation: a) full aircraft geometry; b) surface pressure comparison.

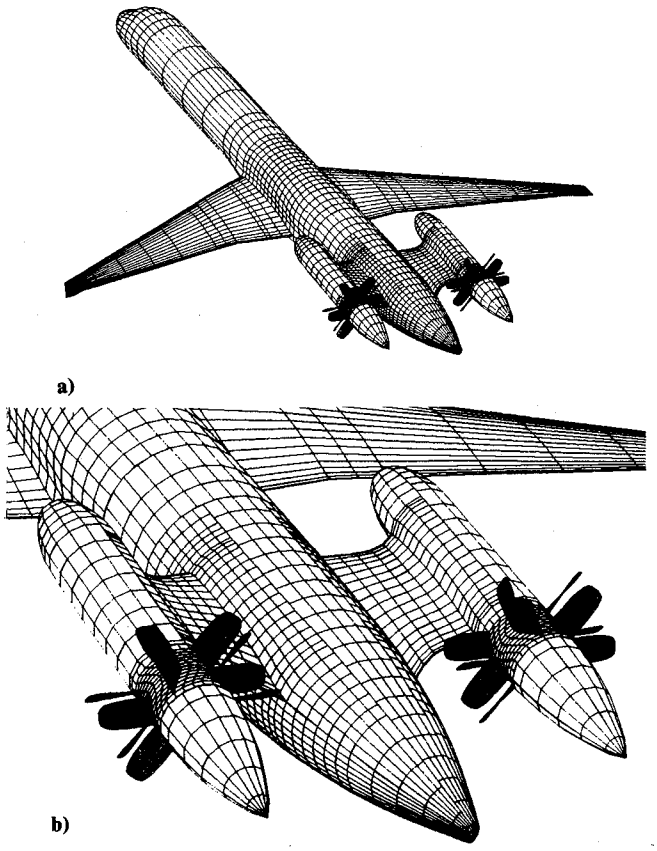

Fig. 14 Counter-rotating configuration: a) full aircraft geometry; b) aft-fuselage detail.

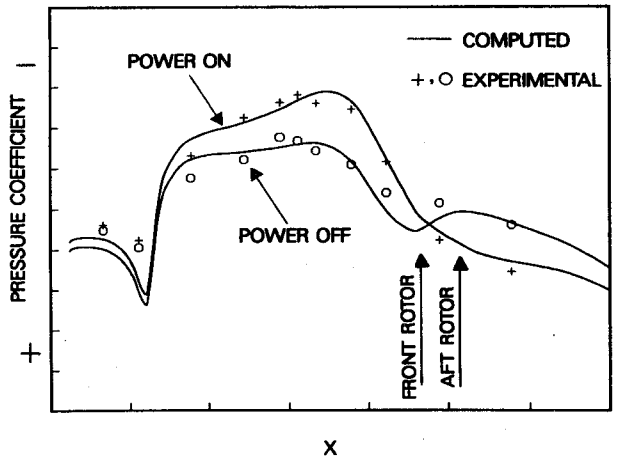

Fig. 15 Result for counter-rotating case.

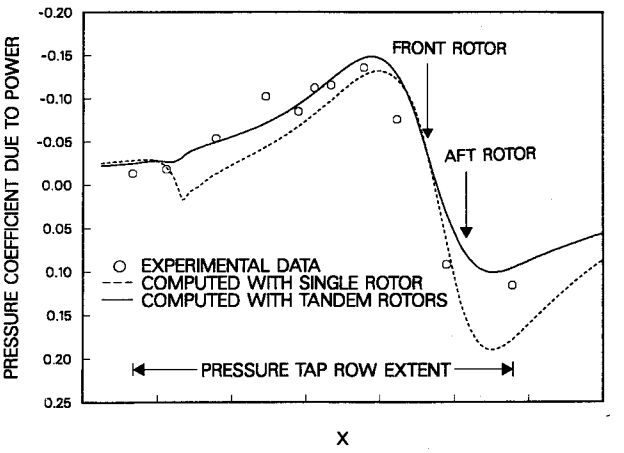

Fig. 16 Surface pressure increments.

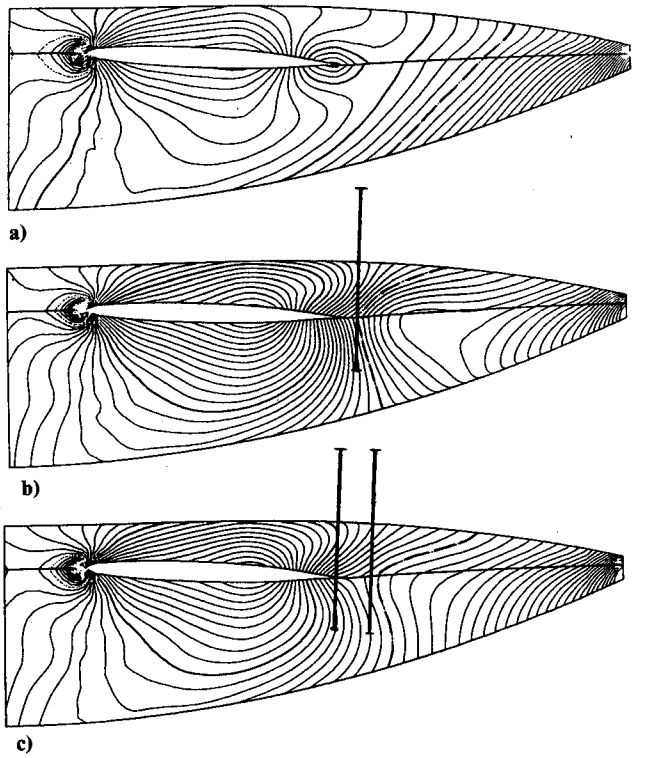

Fig. 17 Computed surface isobars on aft fuselage: a) no propeller; b) single-rotor propeller; c) tandem-rotor propeller.

pressure due to the propulsor are shown in Fig. 16 and demonstrate the new level of accuracy achieved with the present method. It is interesting to point out that the computed thrust loading for the counter-rotating case was several percent lower than that originally input for the single-rotor model (this value was derived from available wind-tunnel measurements). This discrepancy can only serve to highlight that it is not desirable to depend on methods where part of the answer is an input quantity.

Figure 17 shows interesting trends from calculated isobar patterns on the aft-fuselage surface for the geometries of Figs. 13 and 14. As expected, the power-off case shows clear stagnation patterns surrounding the leading and trailing edges of the pylon cutout. The case run with the single-rotor propeller shows the flow around the pylon trailing edge accelerating and then quickly recovering past freestream (dashed line) and remaining at a relatively constant pressure level until the curvature of the tail cone causes further pressure recovery toward stagnation. However, the case run with counter-rotating propellers shows a milder pressure recovery on the aft fuselage, as evidenced by the relative distance between isolines and the location of the line corresponding to freestream (dashed line). These observed trends are very significant because they point to two important conclusions.

1) From an aft-mounted propeller/airframe integration point of view, the counter-rotating propulsor is superior to the single rotor since it subjects the fuselage to less of a power-induced adverse pressure gradient over the aft end of the fuselage (a more adverse gradient could lead to flow separation).

2) From a computational point of view, it is evident that both rotors must be included in the calculations to insure that the propulsor interference is captured correctly.

Figure 18 shows computed streamlines over the aft-fuselage section. These tracings also demonstrate the significant variation of the predicted flow aft of the pylon when all the thrust is generated at one rotor location instead of over two rotors.

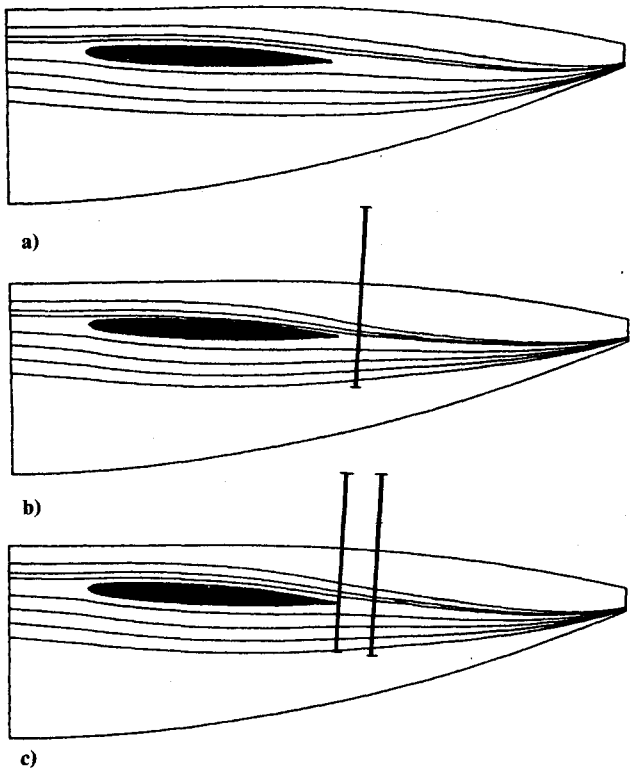

Fig. 18 Computed surface streamlines on aft fuselage: a) no propeller; b) single-rotor propeller; c) tandem-rotor propeller.

Conclusions

A surface panel method for the calculation of isolated and installed multiple-rotor flows has been presented. The method uses a time-averaging technique to simplify the analysis of the complex rotor-to-rotor interaction problem. A technique of superposition is utilized to iteratively compute and account for all rotor influences on any other rotors. Comparisons of computed results with experimental data show excellent agreement and demonstrate this new tool to be a unique capability to address the propulsor/vehicle aerodynamic interference problem.

References

[1]Jou, W. H., "Finite-Volume Calculation of Three-Dimensional Flow Around a Propeller," AIAA Paper 82-0957, June 1982.

[2]Bober, L. J., Chaussee, D. S., and Kutler, P., "Prediction of High-Speed Propeller Flow Fields Using a Three-Dimensional Euler Analysis," AIAA Paper 83-0188, Jan. 1983.

[3]Yamamoto, O., Barton, J. M., and Bober, L. J., "Improved Euler Analysis of Advanced Turboprop Propeller Flows," AIAA Paper 86-1521, June 1986.

[4]Celestina, M. L., Mulac, R. A., and Adamczyk, J. J., "A Numerical Simulation of the Inviscid Flow Through a Counter-Rotating Propeller," NASA TM-87200, June 1986.

[5]Whitfield, D. L., Swafford, T. W., Janus, J. M., Mulac, R. A., and Belk, D. M., "Three-Dimensional Unsteady Euler Solutions for Propfans and Counter-Rotating Propfans in Transonic Flow," AIAA Paper 87-1197, June 1987.

[6]Chen, S. H., and Williams, M. H., "A Panel Method for Counter-Rotating Profans," AIAA Paper No. 87-1890, June 1987.

[7]Hess, J. L., and Valarezo, W. O., "Calculation of Steady Flow About Propellers Using a Surface Panel Method," *Journal of Propulsion and Power*, Vol. 1, No. 6, 1985.

[8]Valarezo, W. O., and Hess, J. L., "Time-Averaged Subsonic Propeller Flowfield Calculations," AIAA Paper 86-1807, June 1986.

[9]Clark, R. W., and Valarezo, W. O., "Subsonic Calculation of Propeller/Wing Interference," AIAA Paper 90-0031, Jan. 1990.

[10]Page, M. A., Ivey, D. M., and Welge, H. R., "Ultra High Bypass Engine Applications to Commercial and Military Aircraft," Society of Automotive Engineers, Warrendale, PA, SAE Paper 861720, Oct. 1986.

[11]Pitera, D. M., Hock, R. W., and Oliver, W. R., "Ultra High Bypass Installation Design for Transport Aircraft," AIAA Paper 87-2280, Aug. 1987.

[12]Vernon, D. F., and Hughes, J. P., "Aerodynamic Integration of Aft-Mounted UHB Propulsion Systems," AIAA Paper 87-2920, Sept. 1987.